ISSN 1615-9306 · JSSCCJ 45 (2) 2022 · Vol. 45 · No. 2 · January 2022

Journal of SEPARATION SCIENCE

2|2022

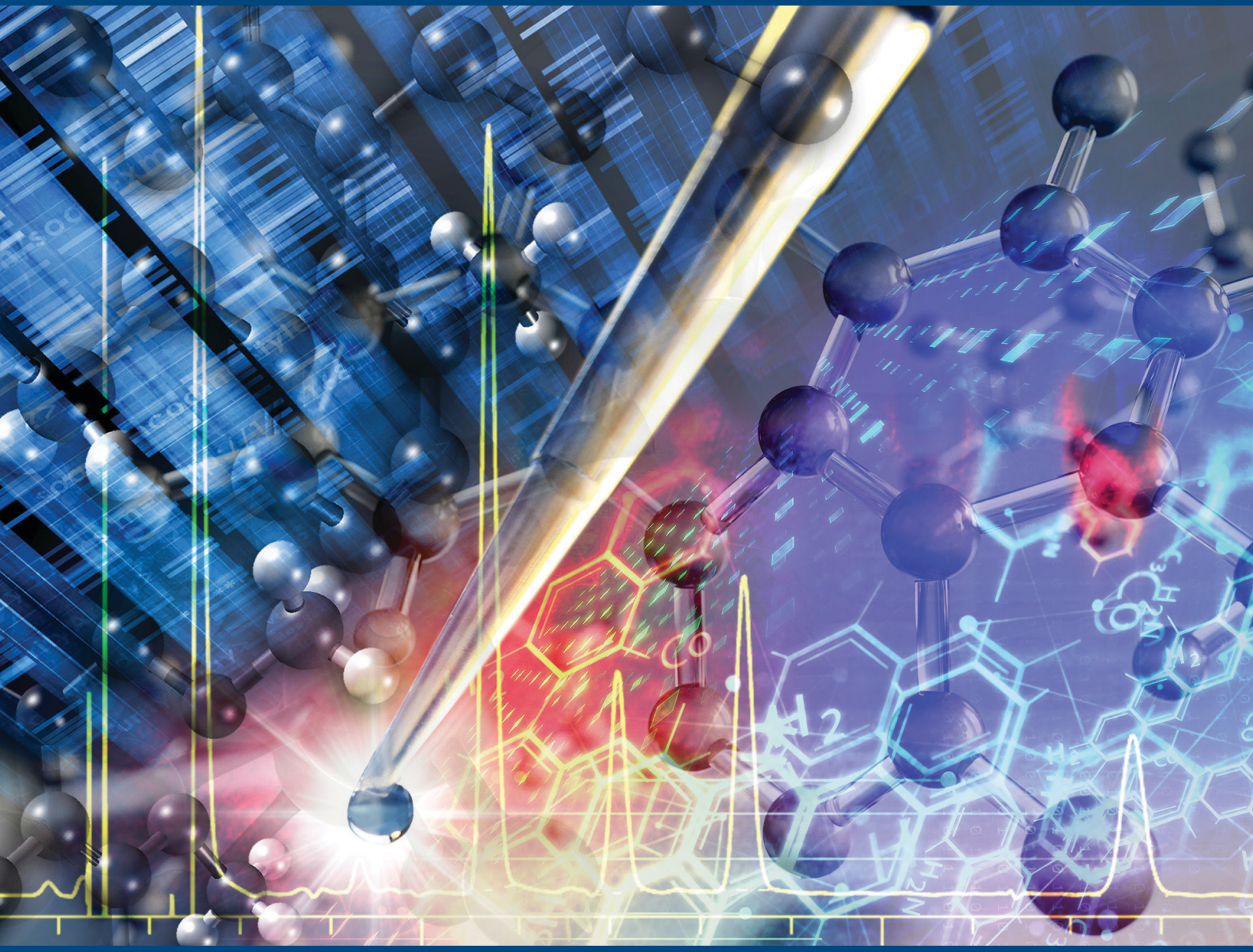

Methods
Chromatography · Electroseparation

Applications
Biomedicine · Foods · Environment

www.jss-journal.com

WILEY-VCH

Received: 20 July 2021 | Revised: 27 October 2021 | Accepted: 27 October 2021

DOI: 10.1002/jssc.202100570

JOURNAL OF SEPARATION SCIENCE

RESEARCH ARTICLE

Investigating interactions between chloroquine/hydroxychloroquine and their single enantiomers and angiotensin-converting enzyme 2 by a cell membrane chromatography method

Qianqian Jia[1,2] | **Jia Fu**[1,2] | **Peida Liang**[1,2] | **Saisai Wang**[1,2] | **Yamin Wang**[1,2] | **Xin Zhang**[1,2] | **Huaxin Zhou**[1,2] | **Liyang Zhang**[1,2] | **Yanni Lv**[1,2] | **Shengli Han**[1,2]

[1] School of Pharmacy, Xi'an Jiaotong University, Xi'an 710061, P. R. China

[2] Institute of Pharmaceutical Science and Technology, Western China Science &Technology Innovation Harbour, Xi'an 710000, P. R. China

Correspondence
Shengli Han, School of Pharmacy, Xi'an Jiaotong University, 76# Yanta West Road, Xi'an 710061, P. R. China.
Email: slhan2008@mail.xjtu.edu.cn

Funding information
National Natural Science Foundation of China, Grant/Award Numbers: 81973278, 81930096; National China Postdoctoral Science Foundation Funded Project, Grant/Award Numbers: 2019T120923, 2018M641003; Natural Science Foundation of Shaanxi Province, Grant/Award Number: 2020SF-309

Chloroquine and hydroxychloroquine have been studied since the early clinical treatment of SARS-CoV-2 outbreak. Considering these two chiral drugs are currently in use as the racemate, high-expression angiotensin-converting enzyme 2 cell membrane chromatography was established for investigating the differences of two paired enantiomers binding to angiotensin-converting enzyme 2 receptor. Molecular docking assay and detection of SARS-CoV-2 spike pseudotyped virus entry into angiotensin-converting enzyme 2-HEK293T cells were also conducted for further investigation. Results showed that each single enantiomer could bind well to angiotensin-converting enzyme 2, but there were differences between the paired enantiomers and corresponding racemate in frontal analysis. *R*-Chloroquine showed better angiotensin-converting enzyme 2 receptor binding ability compared to *S*-chloroquine/chloroquine (racemate). *S*-Hydroxychloroquine showed better angiotensin-converting enzyme 2 receptor binding ability than *R*-hydroxychloroquine/hydroxychloroquine. Moreover, each single enantiomer was proved effective compared with the control group; compared with *S*-chloroquine or the racemate, *R*-chloroquine showed better inhibitory effects at the same concentration. As for hydroxychloroquine, *R*-hydroxychloroquine showed better inhibitory effects than *S*-hydroxychloroquine, but it slightly worse than the racemate. In conclusion, *R*-chloroquine showed better angiotensin-converting enzyme 2 receptor binding ability and inhibitory effects compared to *S*-chloroquine/chloroquine (racemate). *S*-Hydroxychloroquine showed better angiotensin-converting enzyme 2 receptor binding ability than *R*-hydroxychloroquine/hydroxychloroquine (racemate), while the effect of preventing SARS-CoV-2 pseudovirus from entering cells was weaker than *R*-hydroxychloroquine/hydroxychloroquine (racemate).

Article Related Abbreviations: ACE2, angiotensin-converting enzyme 2; CMC, cell membrane chromatography; CQ, chloroquine; HCQ, hydrochloride

KEYWORDS
cell membrane chromatography, chloroquine, hydroxychloroquine, SARS-CoV-2, single enantiomers

1 | INTRODUCTION

Chloroquine (CQ) and hydroxychloroquine (HCQ) are well known as antimalarial drugs introduced in the 1940s [1]. Later, it is discovered that they also have immunomodulatory and anti-inflammatory effects, and are widely used in the treatment of rheumatic diseases, such as rheumatoid arthritis and systemic lupus erythematosus [2–4]. As early as in 1983, CQ has been reported to inhibit influenza A and B viruses [5], and it was found later that CQ has inhibitory effects on replication of human immunodeficiency deficiency virus (HIV) and SARS coronavirus in vitro [6, 7]. As potential broad-spectrum antiviral drugs [8], the use of CQ and HCQ has been widely concerned in the outbreak of SARS-CoV-2. It was reported that CQ could effectively inhibit SARS-CoV-2 replication on Vero E6 cells in vitro at an EC50 value of 1.13 mmol L^{-1} [9], and HCQ was also found to efficiently inhibit SARS-CoV-2 infection in vitro [10]. CQ and HCQ have been used in clinical treatment against the SARS-CoV-2 since February 2020.

The ongoing outbreak of SARS-CoV-2 has caused a large number of deaths and seriously threatened global health security. In the continuous research and study on the virus, angiotensin-converting enzyme 2 (ACE2) was found as an important receptor of SARS-CoV-2 entering the host cells [11–13]. Thus, blocking or antagonizing the ACE2 became a potential strategy of SARS-CoV-2 infection prevention [14, 15]. CQ was found binding to ACE2 with low energy [16], and our previous study also showed that CQ and HCQ could block the ACE2 to prevent the entrance of SARS-CoV-2 pseudovirus into cells [17].

CQ and HCQ are chiral drugs and both are administered as racemates (1:1 mixture of two paired enantiomers of CQ or HCQ). However, they displayed stereoselectivity in their pharmacokinetics properties when used for antimalarial treatment [18]. The potential detrimental cardiac effect and other side effects of CQ and HCQ have been well known for many years [19–21]. These side effects were also reported to be different in enantiomers [22–24]. A lot of separation methods of CQ and HCQ enantiomers were reported, including chiral capillary electrophoresis, supercritical fluid chromatography, and HPLC using chiral columns [25–27]. Among these chromatographic separation methods, HPLC not only analyze quickly and accurately, but also have compatibility with other methods, so it is widely used. Cell membrane chromatography (CMC) maintains the structure and function of membrane proteins making it an effective method for active ingredient screening in complex systems and analysis of receptor–ligand interaction [28, 29]. It was a suitable way to investigate enantiomer difference of CQ and HCQ interacting to ACE2. Stereochemical aspects of CQ and HCQ could thus be exploited to improve clinical safety and efficacy, especially in their use against the SARS-CoV-2 virus [30, 31]. Therefore, the stereoselectivity of CQ and HCQ as antivirus drugs should be investigated.

In this study, a 2D LC system was established to separate enantiomers of CQ/HCQ and evaluate whether a single enantiomer interacts with ACE2 receptor. And the ACE2-HEK293T CMC was used to evaluate the binding affinity of enantiomers acting on ACE2 receptor. We found that *R*-CQ showed better ACE2 receptor binding ability and inhibitory effects compared to *S*-CQ/CQ (racemate). *S*-HCQ showed better ACE2 receptor binding ability than *R*-HCQ/HCQ (racemate), while the effect of preventing SARS-CoV-2 pseudovirus from entering cells was weaker than *R*-HCQ/HCQ (racemate).

2 | MATERIALS AND METHODS

2.1 | Chemicals and reagents

R-chloroquine (*R*-CQ, ≥99%), *S*-CQ (≥98%), *R*-hydroxychloroquine sulfate (*R*-HCQ, ≥98%), and *S*-hydroxychloroquine sulfate (*S*-HCQ, ≥98%) were all purchased from Chengdu Desite Biotech (Chengdu, China). Silica gel (ZEX-II, 5 μm, 200 Å) was purchased from Qingdao Meigao Chemical (Qingdao, China). Methyl tertiary-butyl ether and ethanol (HPLC-grade) were obtained from Thermo Fisher Scientific (Pittsburgh, PA, USA). The purified water was prepared using a Mocell 1810b ultra-pure water system (Chongqing, China). Other reagents were of analytical grade or better.

Cell Counting Kit was purchased from Topscience Biochemical Technology , and the SARS-CoV-2 spike pseudotyped virus (Cat: PSV001) was obtained from Sino Biological (Beijing, China).

2.2 | Instrument and solution preparation

The HPLC system was LC-20AD (Shimadzu, Kyoto, Japan). ACE2-HEK293T/CMC system contained an ACE2-HEK293T/CMC column and an HPLC system (LC-2040C-3D, Shimadzu, Kyoto, Japan). CHIRAL ART Amylose-SA column (250 × 4.6 mm id, YMC Corporation, Japan) was used for the separation of enantiomers. Data acquisition and analysis were carried out using LabSolutions Workstation, and the chromatograms were drawn in GraphPad Prism 6.01. ZL3-2K Speed Vac concentrator (Hunan Kecheng Instrument Equipment , China) was used to evaporate the solvent. Stock solutions of single enantiomer of CQ and HCQ were prepared at the concentration of 1 mmol L^{-1} in methanol and stored at 4°C in the dark. The solutions were diluted to the desired concentrations or filtered with 0.22 μm membrane filters before injection analysis. The stock solutions for experiments at cell level were prepared at the concentration of 80 mmol L^{-1} in DMSO and stored at −20°C in the dark.

2.3 | Separation of enantiomers of chloroquine/hydroxychloroquine and retention on ACE2-HEK293T cell membrane chromatography column

For HPLC system, mobile phase was methyl tertiary-butyl ether–ethanol–diethylamine (98:2:0.1) for CQ or 90:10:0.1 for HCQ at the flow rate of 1.0 mL min^{-1} with the injection volume of 5 μL. The column temperature was maintained at 25°C. For CMC system, sodium chloride solution was used as mobile phase, and the flow rate was 0.2 mL min^{-1}. The column temperature was maintained at 37°C, and the injection volume was 10 μL. The separated single enantiomer (5–6 min for *S*-CQ, 6–7.5 min for *R*-CQ; 5–6.5 min for *R*-HCQ, 9–11 min for *S*-HCQ) was separately collected into four centrifuge tubes, and 10 consecutive injections were collected, merged, and evaporated with a Speed Vac concentrator. Rotation speed was 1500 r/min, and temperature was 25°C. Each enantiomer was dissolved in 100 μL methanol, and filtered with 0.45 μm nylon membrane before the injection into the CMC system.

The ACE2-HEK293T cells were conducted by Genomeditech (Shanghai, China). The cells were cultured in DMEM medium containing 10% fetal bovine serum and 100 U mL^{-1} penicillin. The cells were harvested using trypsin and were washed with the physiological saline. Then, cells (2×10^7) were sonicated in a low osmotic pressure Tris-HCl solution (pH 7.4) at 4°C and cell membrane was separated and obtained by differential centrifugation. Next, the cell membrane suspension was mixed with activated silica (50 mg, 105°C for 30 min) under vacuum. The suspension was stirred for 30 min at 4°C and allowed to stand overnight. Finally, the cell membrane stationary phase was packed into a column (5 × 1 mm id) through the wet packing method. After preparation of the ACE2-HEK293T CMC column, the RSD% value of the retention factor (k) of CQ on the CMC column for three consecutive days was investigated. The reproducibility was also investigated by three consecutive injections on three different columns.

2.4 | Frontal analysis

In order to study the difference of the binding characteristics between each single enantiomer and ACE2, frontal analysis was conducted using ACE2-HEK293T/CMC system. In brief, 51.3 mmol L^{-1} sodium chloride solution was used as mobile phase A, and 51.3 mmol L^{-1} sodium chloride solution added with each enantiomer (10^{-6} mol L^{-1}) was, respectively, used as mobile phase B. ACE2-HEK293T/CMC column was first equilibrated with 100% mobile phase A, and then the mobile phase was switched to a solution that contained a known concentration of enantiomer by adjusting the phase ratio. Each enantiomer solution was continuously applied to the column. When a breakthrough curve was produced, the system was switched back to 100% mobile phase A to elute the analyte from the column.

According to the previous work, frontal analysis of CMC could be used for direct determination of drug–receptor binding interactions by the following reversible equation [32, 33]:

$$\frac{1}{m_{L\mathrm{app}}} = \frac{K_\mathrm{D}}{m_L}\frac{1}{[A]} + \frac{1}{m_L} \quad (1)$$

where $m_{L\mathrm{app}}$ stands for the moles (mol) of analyte required to reach the midpoint of the breakthrough curve at a given molar concentration of analyte, and $[A]$ is the molar concentration of applied analyte. K_D represents the dissociation equilibrium constant for the analyte, which is an important affinity parameter for studying drug–receptor interactions, and m_L is the total moles of binding sites in the column. According to the formula, a plot of $1/m_{L\mathrm{app}}$ versus $1/[A]$ has a linear relationship, and the value of K_D can be calculated by the slope ratio intercept of the linear equation. With the continuous increase of drug concentration, the breakthrough time continues to decrease, and the greater reduction indicates the smaller K_D value.

2.5 | Solvent stoichiometric displacement assay

Solvent stoichiometric displacement experiment was conducted for analyzing the effect of ion concentration on drug–receptor interaction. Briefly, the ACE2-HEK293T/CMC column was equilibrated with a certain concentration buffer and four chiral drug samples were injected. Then, the concentration of buffer was changed, and also samples were injected into the column after it was equilibrated. The retention of each sample under a series of buffer concentrations (10, 11, 12, 13, 14, 15, 16, 17, and 18 mmol L^{-1}) was recorded. According to the stoichiometric displacement theory for retention [34], the equation is given as:

$$\lg k' = \lg I - Z\lg [D], \quad (2)$$

where k' is retention factor of each drug, and $[D]$ stands for the molecular concentration of solvent. Z is the number of solvent molecules released when the solute is adsorbed by the stationary phase, and I is a constant related to the affinity of the solute to the stationary phase. In this experiment, the value of Z reflected the effect of the ion concentration in the mobile phase on the binding of each sample to the stationary phase.

2.6 | Molecular docking assay

Molecular docking study was carried out using the SYBYL-X 2.0 program (Tripos, Missouri, USA). For further study, the influence of the binding of each single enantiomer to ACE2 on the binding of SARS-CoV-2 spike protein to ACE2, the ACE2 structure of PDB: 6M0J was chosen for docking [35]. The structure of ACE2was imported and prepared including removing the water molecules, adding the hydrogen, and minimizing the Pullman charge. The docking results are shown using the ribbon model.

2.7 | Cytotoxicity assay

The ACE2-HEK293T cells were seeded onto 96-well plates (5×10^4 cells per well) and incubated overnight. Then, cells in each well were treated with drug (*R*-CQ or *S*-CQ or *R*-HCQ or *S*-HCQ) in different concentrations (0.1, 1, 10, 25, 50, 100, and 200 μmol L^{-1}) for 24 h. Next, 10 μL Cell Counting Kit solution was added into each well and the cells were incubated for 2 h. The absorbance at 450 nm of each well was measured using a microplate reader (Bio-Rad, Carlsbad, CA, USA). The cells survival rate was calculated using the following formula:

$$Survival\ rate\,(\%) = [(As - Ab)\,/\,(Ac - Ab)] \times 100\% \quad (3)$$

where As is the absorbance of well treated with drugs, Ab is the absorbance of blank medium well seeded with no cells, and Ac represents the absorbance of control well treated with no drugs.

2.8 | Detection of SARS-CoV-2 spike pseudotyped virus entry into ACE2-HEK293T cells

The ACE2-HEK293T cells were seeded onto white 96-well plates (5×10^4 cells in 50 μL medium per well) and incubated at 37°C containing 5% CO_2 atmosphere for 2 h. Note that 25 μL of supernatant of each well was aspirated carefully, and new 25 μL of medium containing certain concentration of drugs was added followed by another 2 h incubation. Then, 5 μL of SARS-CoV-2 spike pseudotyped virus (Sino Biological, PSC001) was added, and cells were incubated for 4 h. After adding complemented medium (100 μL per well) into each well, the plates were placed into the cell incubator for 6–8 h. The supernatant containing the virus was then removed, and fresh medium (200 μL per well) was added. After incubating for 48 h, the culture medium of each well was removed, and cell lysate (20 μL per well) from Luciferase Assay System (Promega, E1500) was added. According to this, after luminescence solution was added (100 μL per well), the luciferase luminescence of each well was detected by a microplate reader under 560 nm.

3 | RESULTS

3.1 | Separation of enantiomers of chloroquine and hydroxychloroquine and retention on ACE2-HEK293T cell membrane chromatography column

The RSD value of the retention factor (k) of CQ on the CMC column for three consecutive days was 8.5%, indicating that the ACE2-HEK293T/CMC column has good activity for at least 3 days. In order to obtain reliable results, each CMC column was used for no more than 3 days. The RSD value of k of CQ on three CMC columns was 6.6% showing the good reproducibility of the column. Besides, the analyte residue of the system was investigated by injecting the solvent into the system, and there was no obvious peak or

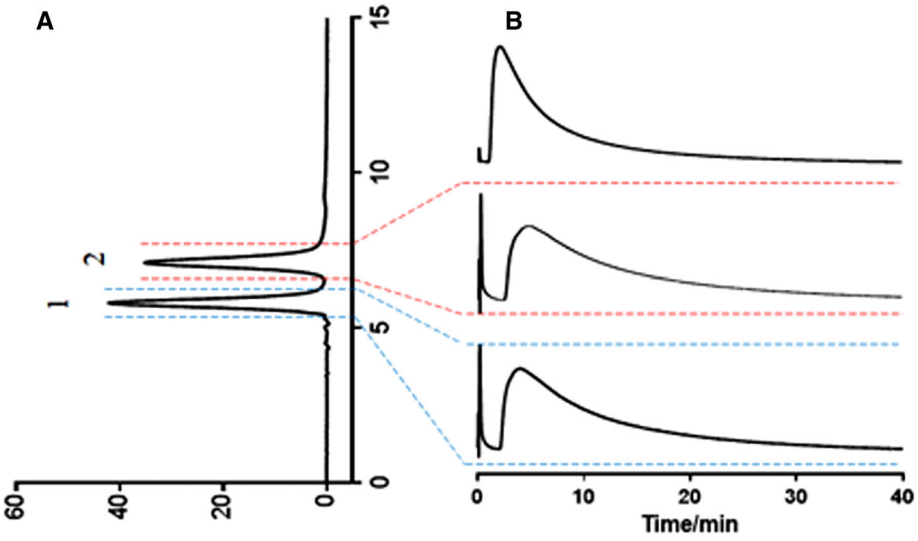

FIGURE 1 Enantiomers separation of chloroquine (CQ) and retention of each enantiomer on ACE2-HEK293T/cell membrane chromatography (CMC) column. (A) Chromatogram of CQ on chiral separation column. Peak 1 was *S*-CQ, and peak 2 was *R*-CQ; (B) retention chromatogram on angiotensin-converting enzyme 2 (ACE2)-HEK293T/CMC column of CQ, *R*-CQ, and *S*-CQ from top to bottom

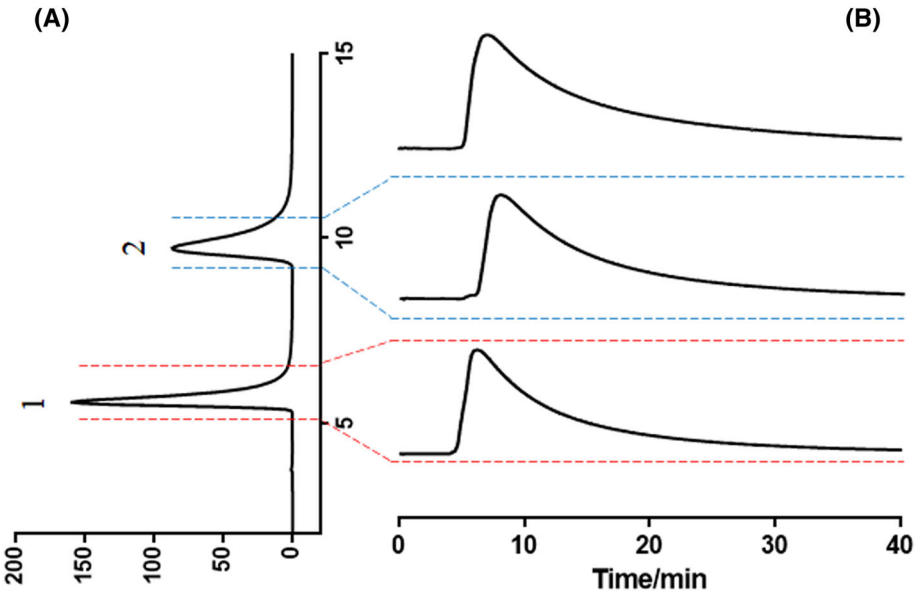

FIGURE 2 Enantiomers separation of hydroxychloroquine (HCQ) and retention of each enantiomer on angiotensin-converting enzyme 2 (ACE2)-HEK293T/cell membrane chromatography (CMC) column. (A) Chromatogram of HCQ on chiral separation column. Peak 1 was *R*-HCQ, and peak 2 was *S*-HCQ; (B) retention chromatogram on ACE2-HEK293T/CMC column of HCQ, *S*-HCQ, and *R*-HCQ from top to bottom

UV absorption wavelength of the sample. The two enantiomers of CQ were separated as shown in Figure 1A, and peak 1 was *S*-CQ and peak 2 was *R*-CQ. Each single enantiomer was enriched and re-dissolved in methanol as the sample injected into the CMC system. As shown in Figure 1B, like the racemate, *S*-CQ and *R*-CQ also displayed retention characteristic on ACE2-HEK293T/CMC column, and it showed no obvious difference with the racemate. Similarly, the chromatogram of HCQ on chiral separation column is shown in Figure 2A. Peak 1 was *R*-HCQ, and peak 2 was *S*-HCQ. Figure 2B also showed that the retention of these two enantiomers on the column was also slightly different. The result showed that enantiomers can be completely separated under the analytical conditions used in the experiment, and each single enantiomer of CQ and HCQ could interact with ACE2.

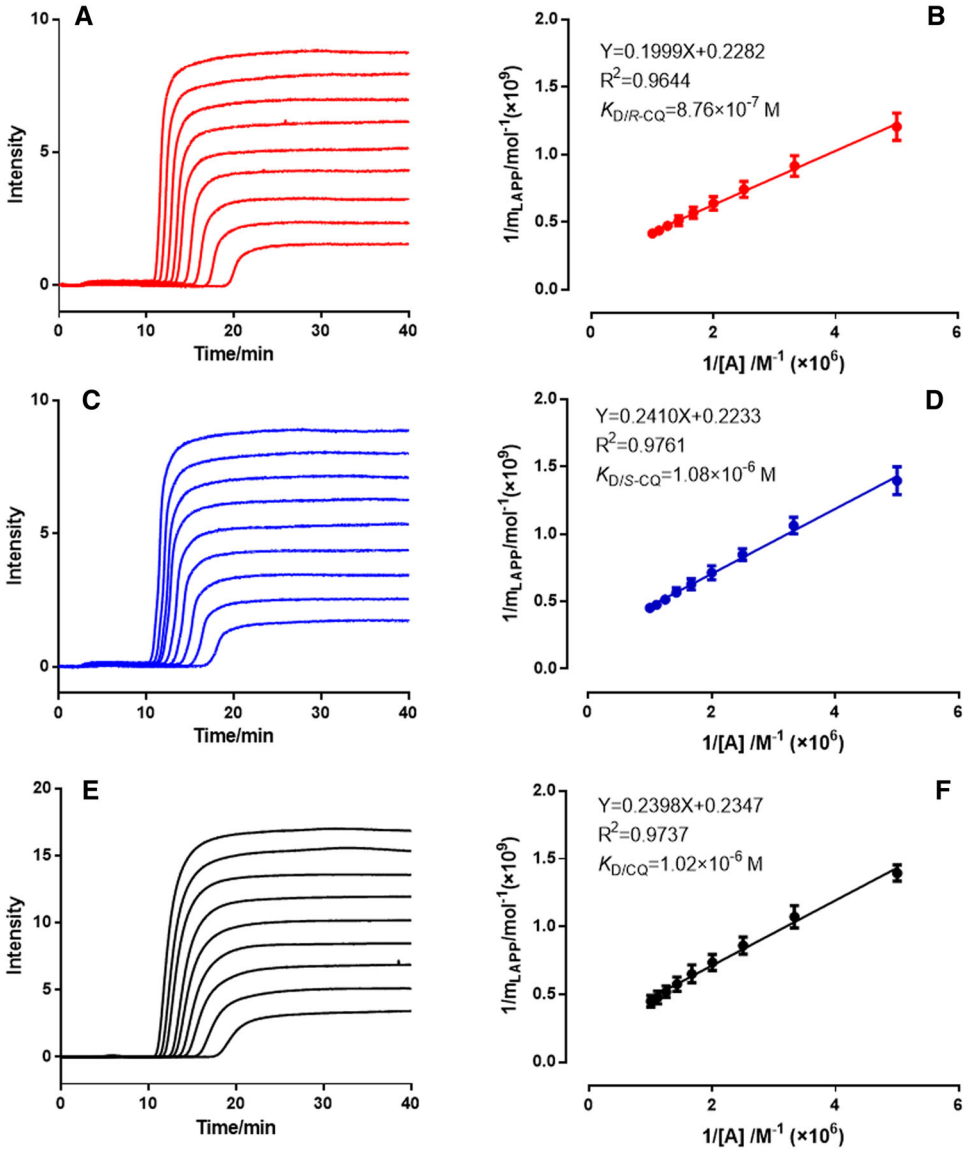

FIGURE 3 Frontal analysis of two enantiomers of chloroquine (CQ) on angiotensin-converting enzyme 2 (ACE2)-HEK293T/cell membrane chromatography (CMC) column. Breakthrough curves of *R*-CQ (A), *S*-CQ (C), and CQ (racemate) (E). The concentrations of *R*-CQ/*S*-CQ/CQ (racemate) were 2×10^{-7}, 3×10^{-7}, 4×10^{-7}, 5×10^{-7}, 6×10^{-7}, 7×10^{-7}, 8×10^{-7}, 9×10^{-7}, and10^{-6} mol L^{-1} from bottom to top, and detection wavelength was 341 nm; a regression curve achieved by plotting $1/m_{L\text{app}}$ versus $1/[A]$ of *R*-CQ (B), *S*-CQ (D), and CQ (racemate) (F). Each point with a bar represents the mean ± SD ($n = 3$)

3.2 | Frontal analysis

Frontal analysis of each enantiomer on ACE2-HEK293T/CMC column was carried out, and the results are shown in Figures 3 and 4. Figure 3A, C, and E shows breakthrough curves of *R*-CQ, *S*-CQ, and CQ (racemate), respectively, and Figure 3B, D, F shows corresponding linear fitting curves of $1/A$ and $1/m_{L\text{app}}$. The dissociation equilibrium constants (K_D) obtained from the model were (8.76 ± 0.51) × 10^{-7} mol L^{-1} for *R*-CQ, (1.08 ± 0.04) × 10^{-6} mol L^{-1} for *S*-CQ, and (1.02 ± 0.17) × 10^{-6} mol L^{-1} for CQ (racemate). The breakthrough curves of two enantiomer and racemate of HCQ are shown in Figure 4A, C, and E, and the corresponding linear fitting are shown in Figure 4B, D, and F. The K_D values were (1.56 ± 0.11) × 10^{-6} mol L^{-1} for *R*-HCQ, (1.08 ± 0.03) × 10^{-6} mol L^{-1} for *S*-HCQ, and (1.20 ± 0.30) × 10^{-6} mol L^{-1} for HCQ (racemate). The differences in K_D value ($K_{D/R\text{-CQ}} < K_{D/\text{CQ (racemate)}} < K_{D/S\text{-CQ}}$) showed that the binding ability of *R*-CQ and ACE2 was stronger than that of *S*-CQ/CQ (racemate). As for HCQ ($K_{D/S\text{-CQ}} < K_{D/\text{HCQ (racemate)}} < K_{D/R\text{-CQ}}$), *S*-HCQ has stronger binding ability with ACE2 than *R*-HCQ/HCQ (racemate). Unlike CQ, the K_D values of the two enantiomers and racemate of HCQ are in the

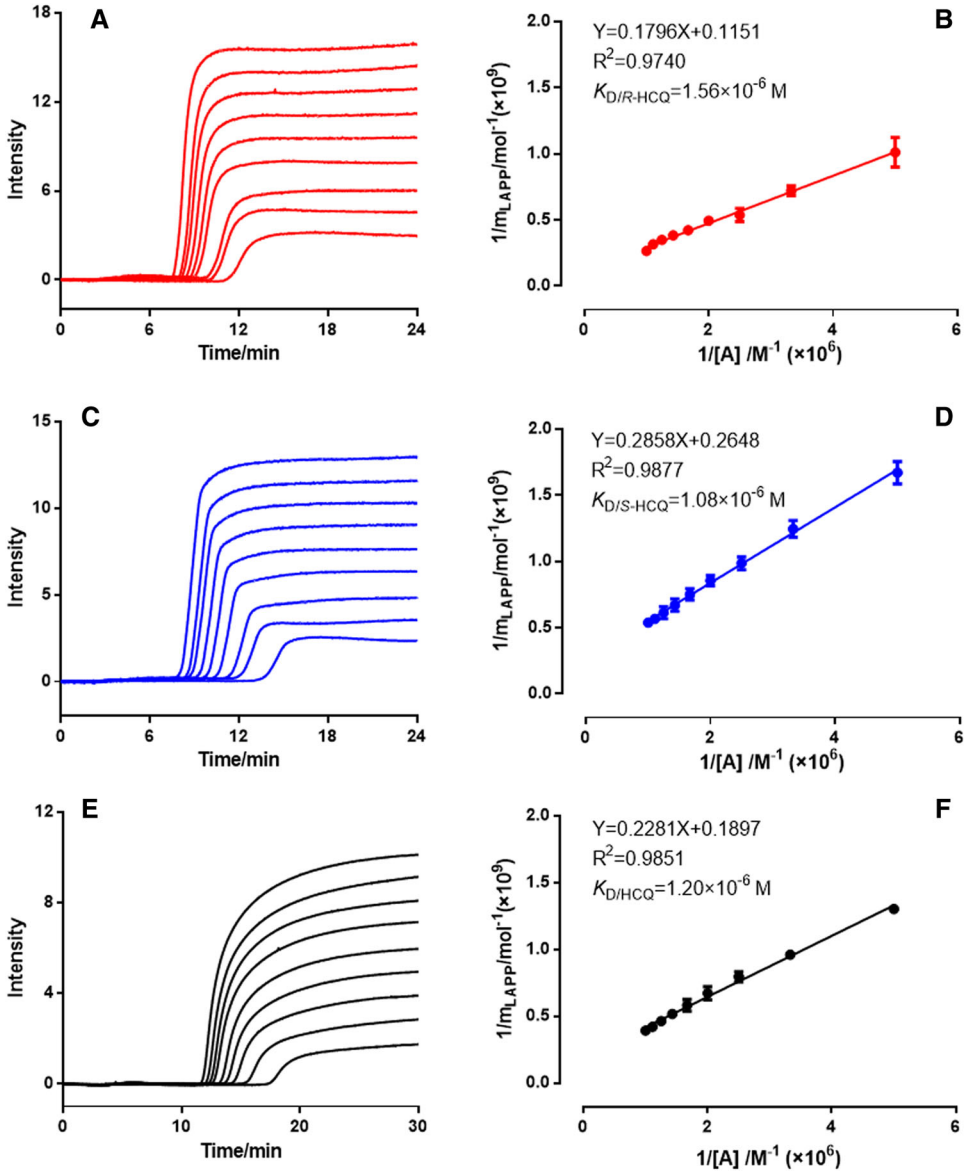

FIGURE 4 Frontal analysis of two enantiomers of hydroxychloroquine (HCQ) on angiotensin-converting enzyme 2 (ACE2)-HEK293T/cell membrane chromatography (CMC) column. Breakthrough curves of *R*-HCQ (A), *S*-HCQ (C), and HCQ (racemate) (E). The concentrations of *R*-HCQ/*S*-HCQ/HCQ (racemate) were 2×10^{-7}, 3×10^{-7}, 4×10^{-7}, 5×10^{-7}, 6×10^{-7}, 7×10^{-7}, 8×10^{-7}, 9×10^{-7}, and 10^{-6} mol L^{-1} from bottom to top, and detection wavelength was 341 nm; a regression curve achieved by plotting $1/m_{L\text{app}}$ versus $1/[A]$ of *R*-HCQ (B), *S*-HCQ (D), and HCQ (racemate) (F). Each point with a bar represents the mean ± SD

same order of magnitude (10^{-6} mol L^{-1}), indicating there was little difference in the strength of binding to ACE2 receptors of these two enantiomers.

3.3 | Solvent stoichiometric displacement assay

The results of solvent stoichiometric displacement assay are shown in Figure 5. Figure 5A shows the results of *R*-CQ, *S*-CQ, and CQ (racemate), and the values of *Z* were 2.635, 2.468, and 2.051, respectively. The values of *Z* were 2.071 for *R*-HCQ, 1.830 for *S*-HCQ, and 2.621 for the racemate of HCQ. The corresponding fitted linearity is shown in Figure 5B. Compared with *S*-enantiomers, *R*-enantiomers of these two drugs caused more solvent molecules released in the process of interacting with the ACE2 receptor on the cell membrane stationary phase ($Z_{R\text{-CQ}} > Z_{S\text{-CQ}} > Z_{\text{CQ (racemate)}}$, $Z_{\text{HCQ (racemate)}} > Z_{R\text{-HCQ}} > Z_{S\text{-HCQ}}$). It showed that *R*-CQ was more susceptible to the ionic strength of the solution than *S*-CQ/CQ (racemate) when interacting with the ACE2, while HCQ (racemate) was more susceptible than *S*-CQ/*R*-HCQ.

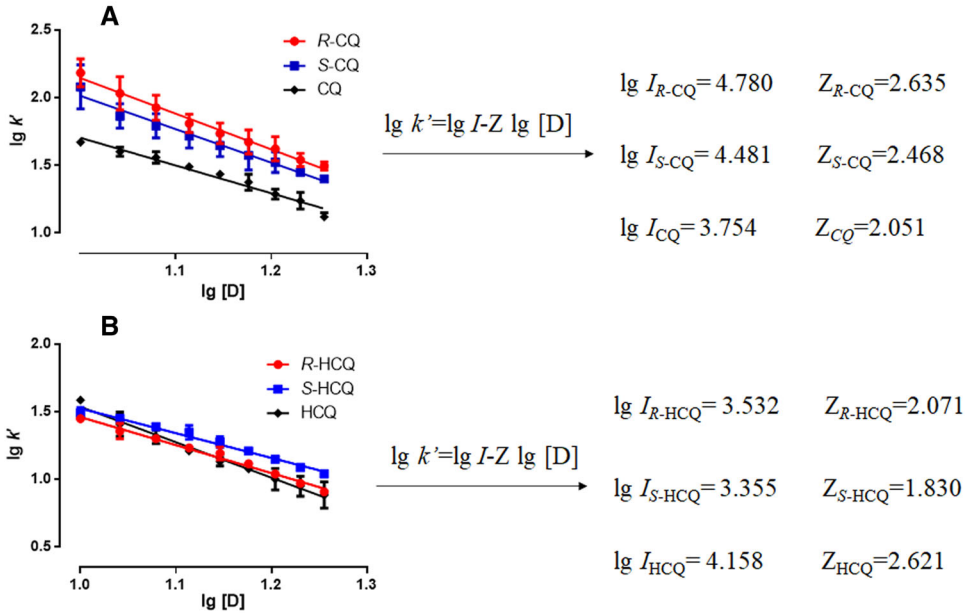

FIGURE 5 Solvent stoichiometric displacement assay of two enantiomers of hydroxychloroquine (HCQ) on angiotensin-converting enzyme 2 (ACE2)-HEK293T/cell membrane chromatography (CMC) column. (A) Regression curves achieved by plotting log*k'* versus log[*D*] of *R*-CQ, *S*-CQ, and chloroquine (CQ) (racemate); (B) regression curve achieved by plotting log*k'* versus log[*D*] of *R*-HCQ, *S*-HCQ, and HCQ (racemate). Each point with a bar represents the mean ± SD ($n = 3$)

3.4 | Molecular docking assay

Molecular docking of *S*-CQ, *R*-CQ, *R*-HCQ, and *S*-HCQ was performed on ACE2 receptor for predicting the predominant binding modes of these drugs with ACE2. The docking results are shown in Figure 6. *R*-CQ and *S*-CQ both could form the hydrogen bond with ASP382, and *R*-CQ could also bond with HIS401 of ACE2. *R*-HCQ formed five hydrogen bonds with THR347, GLU398, GLU402, ARG514, and TRY515, while *S*-HCQ formed three hydrogen bonds with ASP382, ASP350, and ARG393. The specific structure and binding information with ACE2 are summarized in Table 1. Apparently, *S*-CQ, *R*-CQ, *R*-HCQ, and *S*-HCQ could all effectively bind to ACE2, which explained the retention of these four drugs on the ACE2-HEK293T/CMC column. Besides, according to the score value obtained by the built-in scoring function of SYBYL-X 2.0, the total score of the *S*-enantiomer is higher than the corresponding *R*-enantiomer in Table 1, and the difference in the scores of the two enantiomers of CQ was greater than that of HCQ. It indicated that the binding ability of *R*-HCQ and *S*-HCQ with the receptor is not much different, and it could also be seen from the calculated K_D value in the frontal analysis.

3.5 | Cytotoxicity assay

The effects of *S*-CQ, *R*-CQ, *R*-HCQ, and *S*-HCQ on ACE2-HEK293T cell viability were determined following the instructions of the Cell Counting Kit, and results are shown in Figure 7A,B. For *S*-CQ and *R*-HCQ, they had no significant effect on ACE2-HEK293T cell viability when the concentration was less than 10 μmol L^{-1}. For *R*-CQ and *S*-HCQ, the concentration was below 25 μmol L^{-1}. When the concentration of these four drugs was above 50 μmol L^{-1}, the survival rate of ACE2-HEK293T cells was reduced in a dose–dependent manner. It can be concluded that compared with *R*-CQ, *S*-CQ was more toxic to ACE2-HEK293T cells, and *R*-HCQ was more likely to affect cell viability than *S*-HCQ in a lower concentration.

3.6 | Detection of SARS-CoV-2 spike pseudotyped virus entry into ACE2-HEK293T cells

The luciferase luminescence of ACE2-HEK293T infected only with SARS-CoV-2 spike pseudotyped virus was considered as controls, and the value was defined as 1. The drugs at a concentration of 10 μmol L^{-1} were chosen to investigate the differences in the effects on cells infected by pseudotyped virus. The results are shown in Figure 8. It was obvious that four drugs could all reduce the ability of SARS-CoV-2 spike pseudotyped virus to enter ACE2-HEK293T cells, and the percentage of control (PC) were 0.251 ± 0.046 for *R*-CQ, 0.705 ± 0.045 for *S*-CQ, 0.429 ± 0.039 for *R*-HCQ, and 0.690 ± 0.128 for *S*-HCQ. Compared with *S*-CQ, the *R*-CQ showed better inhibitory effects at

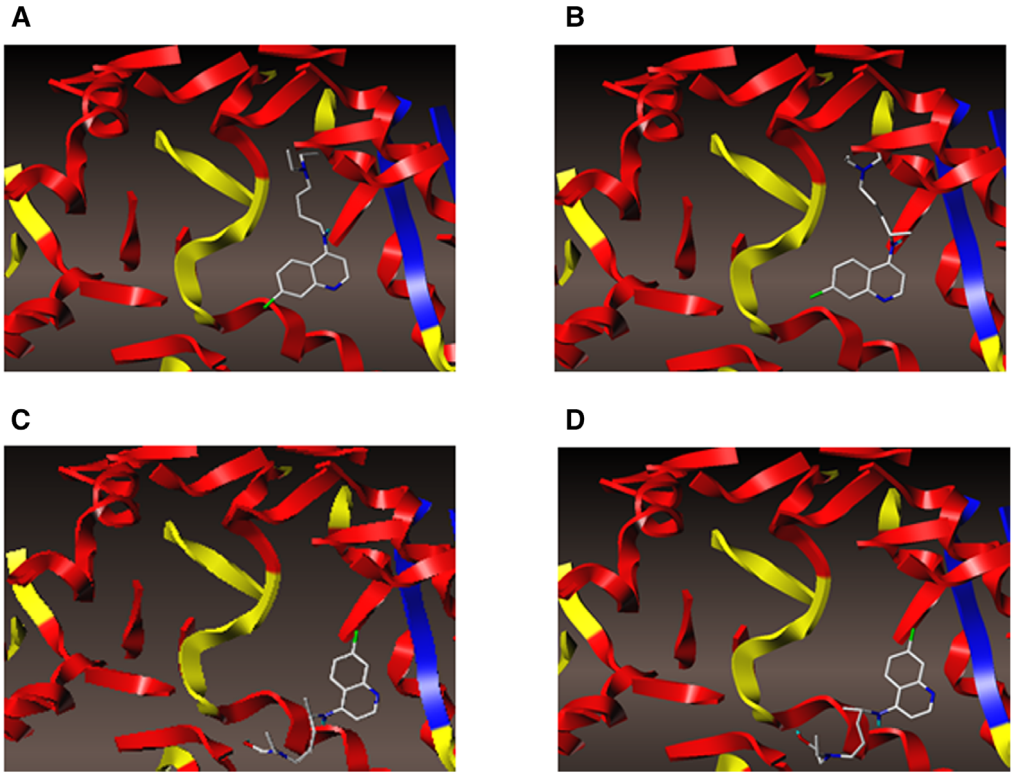

FIGURE 6 Molecular docking modeling of two paired enantiomers with angiotensin-converting enzyme 2 (ACE2). (A) Molecular docking modeling of *R*-CQ with ACE2; (B) molecular docking modeling of *S*-CQ with ACE2; (C) molecular docking modeling of *R*-HCQ with ACE2; (D) molecular docking modeling of *S*-CQ with ACE2

TABLE 1 Specific binding information of two paired enantiomers with angiotensin-converting enzyme 2 (ACE2)

Compound	Structure	Total score	Crash	Polar
R-Chloroquine	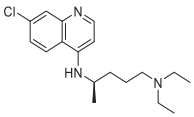	5.83	−0.75	1.44
S-Chloroquine	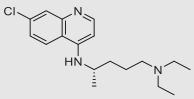	7.53	−0.97	2.41
R-Hydroxychloroquine	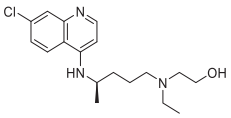	6.46	−0.68	0.46
S-Hydroxychloroquine	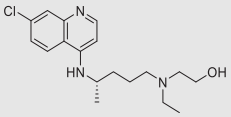	7.49	−0.98	3.40

the same concentration, and it was same for HCQ. Besides, the difference between two enantiomers of CQ was more significant. It indicated that *R*-CQ was more effective in reducing the ability of pseudotyped virus to enter ACE2-HEK293T cells.

4 | DISCUSSION

The frontal analysis and docking results showed that *S*-HCQ has stronger binding ability with ACE2 than *R*-HCQ/HCQ (racemate). Meantime, as the K_D values of

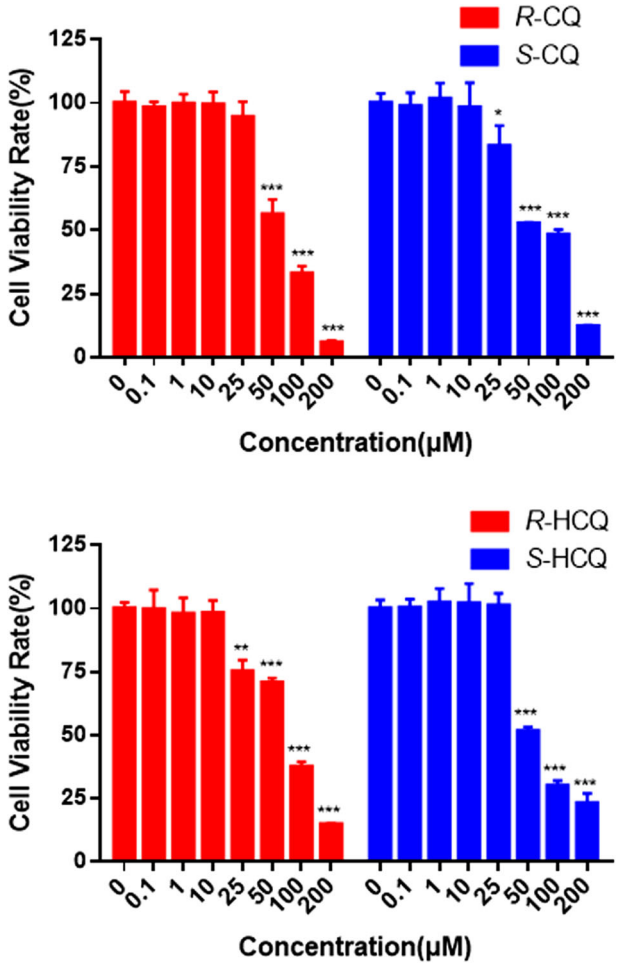

FIGURE 7 Effect of paired enantiomers on viability of angiotensin-converting enzyme 2 (ACE2)-HEK293T cells. Data were presented as mean ± SD ($n = 3$) (*$p < 0.05$; **$p < 0.01$; ***$p < 0.001$ compared with group 0)

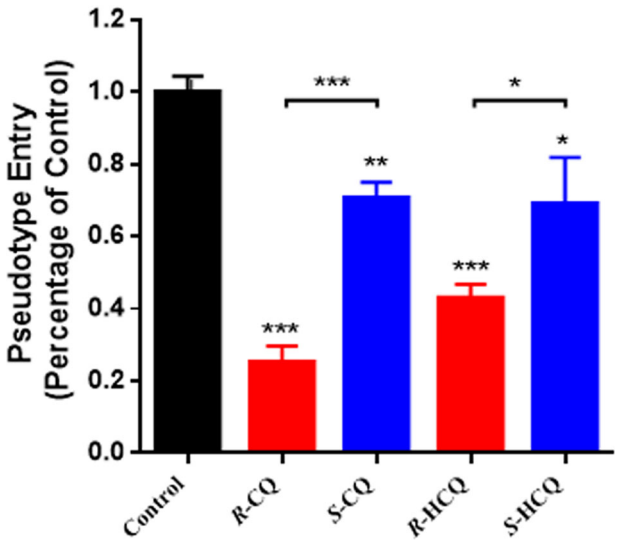

FIGURE 8 Effect of paired enantiomers on the entry of SARS-CoV-2 spike pseudotyped virus into angiotensin-converting enzyme 2 (ACE2)-HEK293T cells. Data were presented as mean ± SD ($n = 3$) (*$p < 0.05$; **$p < 0.01$; ***: $p<0.001$)

R-HCQ, *S*-HCQ, and HCQ (racemate) were in the same order of magnitude (10^{-6} mol L^{-1}), the binding ability of these two enantiomers and the receptor was not much different. According to our previous work, the percentage of control of HCQ (racemate) at 10 mmol L^{-1} in pseudotyped virus entry detection was 0.35 ± 0.0005 [17], while it was 0.429 ± 0.039 for *R*-HCQ, as shown in Figure 8. However, retinopathy, a severe side effect of HCQ was caused by an enantioselective accumulation of the *R*-HCQ enantiomer in the ocular tissue [24], and cytotoxic concentration of *R*-HCQ to ACE2-HEK293T cells was lower than *S*-HCQ, as shown in Figure 7. Therefore, the drug safety of *R*-HCQ has to further be evaluated. Based on the above results, *S*-HCQ has stronger binding ability with ACE2 than *R*-HCQ/HCQ (racemate). Although *S*-HCQ showed no better effects than *R*-HCQ/HCQ (racemate) in pseudotyped virus entry detection experiment, the use of *S*-HCQ instead of HCQ (racemate) is still an option considering the side effect of *R*-HCQ. More experiments of HCQ and its single enantiomers should be conducted taking into account the safety and effectiveness of anti-virus (SARS-Cov-2).

As summarized in Table 2, the order of the strength of the interaction between two enantiomers of CQ and ACE2 was consistent with the preliminary verification results of activity ($K_{D/R\text{-CQ}} < K_{D/CQ\ (racemate)} < K_{D/S\text{-CQ}}$, $PC_{R\text{-CQ}} < PC_{CQ\ (racemate)} < PC_{S\text{-CQ}}$). However, molecular docking results were inconsistent with the results of frontal analysis or the pseudotyped virus infection experiments. It indicated that *R*-CQ/*S*-CQ not only could compete for binding ACE2 regions that bind to spike protein of SARS-CoV-2, but also might make receptor allosteric and affect the binding of ACE2 to spike protein [36]. It seemed that the activity of preventing virus from infecting cells was closely related to their ability to bind to ACE2 receptors. *R*-CQ showed much better activity and safer cytotoxic concentration than *S*-CQ. It hints that the use of a single *R*-CQ may be more effective in preventing SARS-CoV-2 infection of human cells expressing ACE2.

In summary, four drugs could all interact with the ACE2 receptor, showing potential activity to prevent the virus from binding to the ACE2 receptor, and the detections of SARS-CoV-2 spike pseudotyped virus entry verify the ability. It showed that the ACE2-HEK293T/CMC was a reliable method for screening the potential active components. Meantime, *R*-CQ showed better inhibitory effects than *S*-CQ and CQ racemate at the same concentration, and difference between two enantiomers was significant. The binding ability to ACE2 receptor of *S*-HCQ was found better than *R*-HCQ/HCQ (racemate), while the effect of preventing SARS-CoV-2 pseudovirus from entering cells

TABLE 2 Single enantiomer of chloroquine (CQ)/hydroxychloroquine (HCQ) and angiotensin-converting enzyme 2 (ACE2) receptor interaction parameters

Compound	K_D (10^{-7} mol L^{-1})	*Z* value	Docking score	Percentage of control
R-Chloroquine	8.76 ± 0.51	2.635	5.83	0.251 ± 0.046
S-Chloroquine	10.8 ± 0.04	2.468	7.53	0.705 ± 0.045
Chloroquine (racemate)	10.2 ± 0.17	2.051	–	0.44 ± 0.0018[#]
R-Hydroxychloroquine	15.6 ± 0.11	2.071	6.46	0.429 ± 0.039
S-Hydroxychloroquine	10.8 ± 0.03	1.830	7.49	0.690 ± 0.128
Hydroxychloroquine (racemate)	12.0 ± 0.30	2.621	–	0.35 ± 0.0005[#]

[#](a) Data taken from [17]; (b) percentage of control means the SARS-CoV-2 spike pseudotyped virus entrance ratio, and luciferase luminescence value of controls was defined as 1.

was weaker than *R*-HCQ/HCQ (racemate) at the same concentration.

In this study, we established a two-dimensional LC system, which will be a rapid and convenient way to separate enantiomers and evaluate whether a single enantiomer interacts with ACE2 receptor. Meantime, CMC was used to evaluate the binding affinity of enantiomers acting on ACE2 receptor in second dimensional simultaneously. The dissociation equilibrium constants (K_D) of each enantiomer with ACE2 receptor were obtained and compared for the first time. Moreover, the differences in the abilities of the two paired enantiomers to prevent SARS-CoV-2 spike pseudotyped virus from entering cells were first investigated and compared. This study provides a new insight into the use of single enantiomers of CQ/HCQ for SARS-CoV-2 treatment.

ACKNOWLEDGMENTS

This work was supported by the National Natural Science Foundation of China (Grant Numbers: 81973278 and 81930096), National China Postdoctoral Science Foundation Funded Project (Grant Numbers: 2019T120923 and 2018M641003), and Natural Science Foundation of Shaanxi Province (Grant Numbers: 2020SF-309).

CONFLICT OF INTEREST

The authors have declared no conflict of interest.

DATA AVAILABILITY STATEMENT

The data that support the findings of this study are available from the corresponding author upon reasonable request.

ORCID

Shengli Han https://orcid.org/0000-0003-1887-6484

REFERENCES

1. Blackburn CRB. The treatment of malaria. Bull Postgrad Comm Med Univ Syd. 1946;2:183–9.
2. Al-Bari MAA. Chloroquine analogues in drug discovery: new directions of uses, mechanisms of actions and toxic manifestations from malaria to multifarious diseases. J Antimicrob Chemoth. 2015;70:1608–21.
3. Scull E. Chloroquine and hydroxychloroyuine therapy in rheumatoid arthritis. Arthritis Rheum. 1962;5:30–6.
4. Costedoat-Chalumeau N, Amoura Z, Hulot JS, Lechat P, Piette JC. Hydroxychloroquine in systemic lupus erythematosus. Lancet 2007;369:1257–8.
5. Shibata M, Aoki H, Tsurumi T, Sugiura Y, Nishiyama Y, Suzuki S, Maeno K. Mechanism of uncoating of influenza B virus in MDCK cells: action of chloroquine. J Gen Virol. 1983;64:1149–56.
6. Pardridge WM, Yang J, Diagne A. Chloroquine inhibits HIV-1 replication in human peripheral blood lymphocytes. Immunol Lett. 1998;64:45–7.
7. Vincent MJ, Bergeron E, Benjannet S, Erickson BR, Rollin PE, Ksiazek TG, Seidah NG, Nichol ST. Chloroquine is a potent inhibitor of SARS coronavirus infection and spread. Virol J. 2005;2:69.
8. Savarino A, Di Trani L, Donatelli I, Cauda R, Cassone A. New insights into the antiviral effects of chloroquine. Lancet Infect Dis. 2006;6:67–9.
9. Wang M, Cao R, Zhang L, Yang X, Liu J, Xu M, Shi Z, Hu Z, Zhong W, Xiao G. Remdesivir and chloroquine effectively inhibit the recently emerged novel coronavirus (2019-nCoV) in vitro. Cell Res. 2020;30:269–71.
10. Liu J, Cao R, Xu M, Wang X, Zhang H, Hu H, Li Y, Hu Z, Zhong W, Wang M. Hydroxychloroquine, a less toxic derivative of chloroquine, is effective in inhibiting SARS-CoV-2 infection in vitro. Cell Discov. 2020;6:16.
11. Hoffmann M, Kleine-Weber H, Schroeder S, Krüger N, Herrler T, Erichsen S, Schiergens TS, Herrler G, Wu NH, Nitsche A, Müller MA, Drosten C, Pöhlmann S. SARS-CoV-2 cell entry depends on ACE2 and TMPRSS2 and is blocked by a clinically proven protease inhibitor. Cell 2020;181:271–80.e8.
12. Letko M, Marzi A, Munster V. Functional assessment of cell entry and receptor usage for SARS-CoV-2 and other lineage B betacoronaviruses. Nat Microbiol. 2020;5:562–9.
13. Clausen TM, Sandoval DR, Spliid CB, Pihl J, Perrett HR, Painter CD, Narayanan A, Majowicz SA, Kwong EM, McVicar RN, Thacker BE, Glass CA, Yang Z, Torres JL, Golden GJ, Bartels PL, Porell RN, Garretson AF, Laubach L, Feldman J, Yin X, Pu Y, Hauser BM, Caradonna TM, Kellman BP, Martino C, Gordts PLSM, Chanda SK, Schmidt AG, Godula K, Leibel SL,

Jose J, Corbett KD, Ward AB, Carlin AF, Esko JD. SARS-CoV-2 infection depends on cellular heparan sulfate and ACE2. Cell 2020;183:1043–57.e15.
14. Wu Y, Wang F, Shen C, Peng W, Li D, Zhao C, Li Z, Li S, Bi Y, Yang Y, Gong Y, Xiao H, Fan Z, Tan S, Wu G, Tan W, Lu X, Fan C, Wang Q, Liu Y, Zhang C, Qi J, Gao GF, Gao F, Liu L. A noncompeting pair of human neutralizing antibodies block COVID-19 virus binding to its receptor ACE2. Science 2020;368:1274–8.
15. Terali K, Baddal B, Gülcan HO, Prioritizing potential ACE2 inhibitors in the COVID-19 pandemic: insights from a molecular mechanics-assisted structure-based virtual screening experiment. J Mol Graph Model. 2020;100:107697.
16. Abdelli I, Hassani F, Brikci SB, Ghalem S. In silico study the inhibition of angiotensin converting enzyme 2 receptor of COVID-19 by ammoides verticillata components harvested from Western Algeria. J Biomol Struct Dyn. 2021;39:3263–76.
17. Wang N, Han S, Liu R, Meng L, He H, Zhang Y, Wang C, Lv Y, Wang J, Li X, Ding Y, Fu J, Hou Y, Lu W, Ma W, Zhan Y, Dai B, Zhang J, Pan X, Hu S, Gao J, Jia Q, Zhang L, Ge S, Wang S, Liang P, Hu T, Lu J, Wang X, Zhou H, Ta W, Wang Y, Lu S, He L. Chloroquine and hydroxychloroquine as ACE2 blockers to inhibit viropexis of 2019-nCoV spike pseudotyped virus. Phytomedicine 2020;79:153333.
18. Brocks DR, Mehvar R. Stereoselectivity in the pharmacodynamics and pharmacokinetics of the chiral antimalarial drugs. Clin Pharmacokinet. 2003;42:1359–82.
19. Frisk-Holmberg M, Bergqvist Y, Englund U. Chloroquine intoxication. Br J Clin Pharmaco. 1983;15:502–3.
20. Baguet JP, Tremel F, Fabre M. Chloroquine cardiomyopathy with conduction disorders. Heart 1999;81:221–3.
21. Costedoat-Chalumeau N, Hulot JS, Amoura Z, Leroux G, Lechat P, Funck-Brentano C, Piette JC. Heart conduction disorders related to antimalarials toxicity: an analysis of electrocardiograms in 85 patients treated with hydroxychloroquine for connective tissue diseases. Rheumatology 2007;46:808–10.
22. Ofori-Adjei D, Ericsson O, Lindström B, Sjöqvist F. Protein binding of chloroquine enantiomers and desethylchloroquine. Br J Clin Pharmaco. 1986;22:356–8.
23. Haberkorn A, Kraft HP, Blaschke G. Antimalarial activity of the optical isomers of chloroquine diphosphate. Tropenmed Parasitol. 1979;30:308–12.
24. Ducharme J, Fieger H, Ducharme MP, Khalil SK, Wainer IW. Enantioselective disposition of hydroxychloroquine after a single oral dose of the racemate to healthy subjects. Br J Clin Pharmaco. 1995;40:127–33.
25. Moraes de Oliveira AR, Sueli Bonato P. Stereoselective determination of hydroxychloro-quine and its major metabolites in human urine by solid-phase microextraction and HPLC. J Sep Sci. 2007;30:2351–9.
26. Wilson LJ, Mi C, Kraml CM. A preparative chiral separation of hydroxychloroquine using supercritical fluid chromatography. J Chromatogr A. 2020;1634:461661.
27. Lammers I, Buijs J, Ariese F, Gooijer C. Sensitized enantioselective laser-induced phosphorescence detection in chiral capillary electrophoresis. Anal Chem. 2010;82:9410–7.
28. Lin Y, Xu J, Qi J., Sun W, Fu J, Lv Y, Han S. Cell membrane chromatography coupled online with LC-MS to screen anti-anaphylactoid components from *Magnolia biondii* Pamp. targeting on Mas-related G protein-coupled receptor X2. J Sep Sci. 2020;43:2571–8.
29. Wang N, Zhang Q, Xin H, Shou D, Qin L. Osteoblast cell membrane chromatography coupled with liquid chromatography and time-of-flight mass spectrometry for screening specific active components from traditional Chinese medicines. J Sep Sci. 2017;40:4311–9.
30. D'Acquarica I, Agranat I. Chiral switches of chloroquine and hydroxychloroquine: potential drugs to treat COVID-19. Drug Discov Today. 2020;25:1121–3.
31. Lentini G, Cavalluzzi MM, Habtemariam S. COVID-19, chloroquine repurposing, and cardiac cafety concern: chirality might help. Molecules 2020;25:1834.
32. Anguizola J, Joseph KS, Barnaby OS, Matsuda R, Alvarado G, Clarke W, Cerny RL, Hage DS. Development of affinity microcolumns for drug-protein binding studies in personalized medicine: interactions of sulfonylurea drugs with in vivo glycated human serum albumin. Anal Chem. 2013;85:4453–60.
33. Ma W, Zhang D, Li J, Che D, Liu R, Zhang J, Zhang Y. Interactions between histamine H-1 receptor and its antagonists by using cell membrane chromatography method. J Pharm Pharmacol. 2015;67:1567–74.
34. Geng X, Regnier FE. Stoichiometric displacement of solvent by non-polar solutes in reversed-phase liquid chromatography. J Chromatogr A. 1985;332:147–68.
35. Lan J, Ge J, Yu J, Shan S, Zhou H, Fan S, Zhang Q, Shi X, Wang Q, Zhang L, Wang X. Structure of the SARS-CoV-2 spike receptor-binding domain bound to the ACE2 receptor. Nature 2020;581:215–20.
36. Celık̇ I, Onay-Besıkcı̇ A, Ayhan-Kilcigil̇ G. Approach to the mechanism of action of hydroxychloroquine on SARS-CoV-2: a molecular docking study. J Biomol Struct Dyn. 2021;39:5792–8.

How to cite this article: Jia Q, Fu J, Liang P, Wang S, Wang Y, Zhang X, Zhou H, et al. Investigating interactions between chloroquine/hydroxychloroquine and their single enantiomers and angiotensin-converting enzyme 2 by a cell membrane chromatography method. J Sep Sci. 2022;45:456–467.
https://doi.org/10.1002/jssc.202100570